applied sciences

Article

Method for Calculating Vertical Compression Bearing Capacity of the Static Drill Rooted Nodular Pile

Jing Guo [1], Guoliang Dai [2,*] and Yue Wang [3]

[1] Jiang Su Jiao Shui Jian Intelligent Equipment Research Institute, Nanjing 211500, China; twinkleguojing@foxmail.com
[2] School of Civil Engineering, Southeast University, Nanjing 211189, China
[3] Nanjing Iron & Steel United Co., Ltd., Nanjing 211500, China; olivia45nk@163.com
* Correspondence: daigl@seu.edu.cn

Abstract: The static drill rooted nodular (SDRN) pile is a new kind of composite pile foundation made by inserting a precast nodular pile into the cemented soil. Based on the tests and analysis on the mechanism characteristics of these two kinds of interfaces, which are between the pile and cemented soil, and between the cemented soil and soil, this paper proposes a calculation method for the ultimate vertical bearing capability of the SDRN pile considering two failure modes. When the precast pile and surrounding cemented soil fails as a whole, the diameter of the cemented soil pile is taken to calculate the ultimate shaft resistance, and the shaft resistance of the SDRN pile is about 1.05∼1.10 times that of the bored pile in the same soil layer. When the core precast pile fails in penetration mode, the diameter of the core pile is taken. The pile shaft resistance takes that of displacement piles in the same soil layer. The lower nodular pile shaft resistance should consider the squeezing effect of nodular joints. Besides, the improvement of pile tip resistance due to the expanded cemented soil should also be taken into consideration. The result is the smaller value calculated according to these two failure modes. The ultimate bearing capacity of a SDRN pile calculated by the theoretical method is not only compared with the field test result, but also the simulation result of a 2D model pile built by PLAXIS finite element software. In addition, the finite element simulation is also confirmed to be an effective way to investigate the mechanism characteristics of SDRN piles more thoroughly.

Keywords: static drill rooted nodular pile; failure mode; shaft resistance; tip resistance; self-balance method; PLAXIS; two-dimensional model

Citation: Guo, J.; Guoliang, D.; Wang, Y. Method for Calculating Vertical Compression Bearing Capacity of the Static Drill Rooted Nodular Pile. *Appl. Sci.* **2022**, *12*, 5101. https://doi.org/10.3390/app12105101

Academic Editor: Daniel Dias

Received: 18 April 2022
Accepted: 14 May 2022
Published: 18 May 2022

1. Introduction

The static drill rooted nodular (SDRN) pile is a new kind of composite pile foundation. The upper section of the SDRN pile is prestressed reinforcement high-intensity concrete pile or prestressed high-intensity concrete pipe (PRHC or PHC) pile, the lower section is a prestressed nodular concrete pile. The static drill rooted method is environment friendly which almost produces no squeezing effect to surrounding foundation. Considering the interaction between the pile, cemented soil, and surrounding soil, the bearing capacity of SDRN pile is improved effectively. In addition, the diameter of cemented soil shell approaching the pile tip is expanded to improve the pile tip performance.

The SDRN pile was introduced from Japan in recent years. To study the vertical load transfer mechanism and bearing capacity of the SDRN pile, many scholars have carried out a series of field tests and numerical simulations analyzed by ABAQUS [1–3]. Due to the similar construction method, the SDRN piles are usually compared with bored piles [3–6]. Meanwhile, the influence of nodular joints and cemented soil on vertical bearing characteristics are also investigated [1–3,5,7,8]. However, few studies focus on the calculation theory of the ultimate compression bearing capacity of single SDRN pile considering the failure mode.

Based on the study of mechanism characteristics of SDRN piles and the calculation theory of similar composite piles, this paper proposes the calculation method of vertical bearing capacity of SDRN pile. The calculation method is verified by the No. 1 line of Ningbo Rail Transit Engineering, which adopts two SDRN piles in the field. Instead of Abaqus, this paper chooses Plaxis to build a 2D model, which is more effective and considerate.

2. Bearing Mechanism of the SDRN Pile

The vertical ultimate bearing capacity of SDRN pile consists of the ultimate shaft and tip resistance. The ultimate shaft resistance consists of the upper section (PRHC or PHC pile) and the lower section (nodular pile).

2.1. Pile Side Bearing Mechanism

For the upper section, the vertical load is transmitted to the surrounding soil through the cemented soil around pile shaft, which is the load double diffusion mode. The cemented soil plays the role of stress transmission, instead of sharing the load directly [9–11]. For the lower section, due to the squeezing effect of nodular joints, the bonding effect between pile and exterior cemented soil is enhanced, approximating deformation compatibility [6].

2.2. Pile Tip Bearing Mechanism

The expansion and solidification of the cemented soil approaching pile tip also affects the bearing capacity. Through field tests [6] and numerical simulations [8], it is found that the axial force in the expanded section decreases acceleratedly and that of the cemented soil increases obviously. In addition, the relative displacement between pile and cemented soil is small. It shows that this kind pile tip can improve the bearing capacity efficiently.

2.3. Existing Calculation Method for Bearing Capacity of SDRN Pile

The standard value of vertical ultimate bearing capacity of SDRN pile is given by [12]

$$Q_{uk} = Q_{sk} + Q_{pk} = \sum u_i q_{sik} l_i + q_{pk} A_p, \tag{1}$$

where Q_{uk} is the standard value of vertical ultimate bearing capacity of SDRN pile, Q_{sk} is the standard value of pile shaft resistance, Q_{pk} is the standard value of pile tip resistance, u_i is the circumference of pile shaft (the nodular pile is calculated according to the outer diameter of nodular joint, and the other types of piles are calculated according to the outer diameter); q_{sik} is the standard value of ultimate pile shaft resistance in the i-th soil layer, which could refer to the field value of precast pile; l_i is the thickness of the i-th layer soil or rock around pile (the shaft resistance among 2 m from pile tip is not included); q_{pk} is the standard value of ultimate pile tip resistance, which could be taken as two-thirds of the field value of precast pile, and A_p is the projected area of the extended pile tip.

Equation (1) suggests that the failure of PRHC or PHC pile may occur between the pile shaft and cemented soil, while that of the nodular pile may happen in the cemented soil around.

3. Failure Modes of the SDRN Pile

There are three pairs of interfaces, which are between the pipe pile and inner cemented soil core, the pipe pile and exterior cemented soil shell, the cemented soil shell and surrounding soil. The bonding strength of the interface between pipe pile and inner cemented soil core is high enough to take them as a whole [4]. Based on the following theoretical and experimental analysis, there are two kinds of shaft resistance failure modes. One is the failure occurs between the pile and exterior cemented soil shell, and the other is between the cemented soil and surrounding soil.

3.1. Overall Failure Mode

Several field tests and model tests have been conducted to study the bearing mechanism of SDRN pile. It is concluded that when the thickness of cemented soil around the pile is within a certain range [4,7]: $1.175r \leq R \leq 2r + 75$ mm (R is radius of the cemented soil pile, and r is outside radius of the pipe pile), the shaft shear failure usually occur between cemented soil and surrounding soil, that is, the pile and surrounding cemented soil fail as a whole. Xu [1] found that the ultimate shaft resistance on the interface between pipe pile and cemented soil is much larger than that on the interface between cemented soil and sandy soil through shear tests. By field tests and model tests, Zhou [6,7] also found that, compared with bored piles, the bearing capacity of pile shaft mainly depends on the shear resistance between cemented soil and surrounding soil. The overall failure mode is shown in Figure 1a.

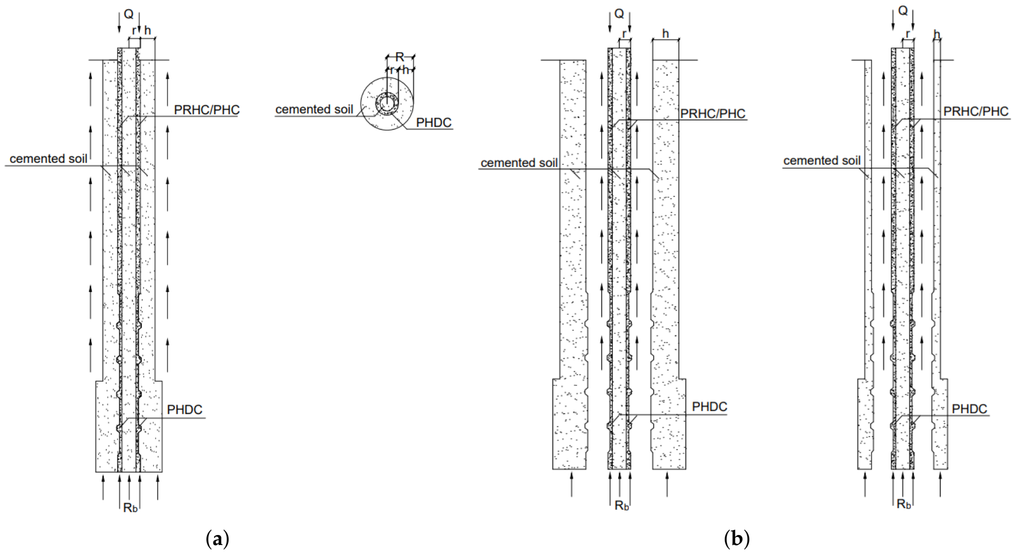

Figure 1. Two failure modes of SDRN pile: (**a**) overall failure mode (pile-cemented soil composite model) and (**b**) core pile penetration failure mode (cemented soil-soil composite model), where Q is the vertical load, and h is the thickness of cemented soil.

3.2. Core Pile Penetration Failure Mode

The field tests and model tests reveal that [4] the shaft shear failure may also happen between pile and exterior cemented soil if the thickness of cemented soil shell is too small or too large, which is the core pile penetration failure mode. The reason is that, compared with the expanded section at pile tip, the thin exterior cemented soil shell may have little influence on pile shaft resistance. In addition, the high moisture content in the upper soft soil layer will also decrease the strength of cemented soil. Both will lead to the shear failure between pile and cemented soil due to difference in stiffness [9]. On the other hand, with the same diameter of exterior cemented soil pile, the thicker the cemented soil shell is, the lower the vertical stiffness is. The high shear force between pile and cemented soil could offset the cohesion before the failure of cemented soil [2], which will also cause the core pile penetration failure.

Through the finite element simulation, Yang [5] found that the stress distribution in a certain range is influenced by joints, about two to three times the diameter of pile near the nodular joint. In particular, the empty area formed by the micro-deformation of squeezed cemented soil will decrease the interface area between pile and cemented soil. As a result, the coefficient η_z should be proposed to take the impact of joints on shaft bearing capacity into consideration. The core pile penetration failure mode is shown in Figure 1b.

4. Calculation Method for Vertical Bearing Capacity of SDRN Pile

4.1. Calculation Method for Overall Failure Mode

On the basis of the analysis above, when the pile and exterior cemented soil shell fail as a whole, the calculation method of MC pile can be referred to. The MC pile is constructed by drilling the precast pile into cemented soil. The pile shaft resistance is calculated according to the diameter of exterior cemented soil pile. The calculation formula for the characteristic value of compression bearing capacity of MC pile is as follows [13]:

$$R_a = u_p \sum \xi_{si} q_{sia} l_i + \xi_p q_{pa} A_p, \tag{2}$$

where u_p is the perimeter of the exterior cemented soil pile, ξ_{si} is the adjustment coefficient of the composite pile shaft resistance, q_{sia} is the characteristic value of the cemented soil pile shaft resistance in the i-th soil layer, l_i is the thickness of the i-th layer of soil or rock around the pile, ξ_p is the adjustment coefficient of composite pile tip resistance, q_{pa} is the characteristic value of the pile tip resistance of the cemented soil pile, and A_p is the projected area of the pile tip.

The SDRN method is to insert SDRN pile into cemented soil. In detail, Qian [4] found, the insertion has three effects on the cemented soil and the surrounding soil by observing the excavated pile: (1) compaction effect on the upper high compressibility soil layers; (2) infiltration into the sizable pores in the lower soil layers; (3) increase of the density and elasticity modulus of the cemented soil around the lower section of pile. Based on the field tests and model tests [3,6], the performance of shear resistance on the interface between cemented soil and surrounding soil is better than that on the interface between bored pile and surrounding soil. The ultimate shear resistance provided by each soil layer around the pile is approximate 1.05∼1.10 times that of the bored pile. Therefore, the standard value q_{sik} of the cemented soil pile shaft resistance in the i-th soil layer is 1.05∼1.10 times that of the bored pile.

$$Q_{sk1} = u_p \sum \eta_1 q_{sik} l_i, \tag{3}$$

where Q_{sk1} is the standard value of pile shaft resistance in overall failure mode, η_1 = 1.05∼1.1 is the coefficient of cemented soil pile shaft resistance considering the squeezing effect; u_p is the perimeter of cemented soil pile not expanded, q_{sik} is the standard value of ultimate cemented soil pile shaft resistance in the i-th soil layer, which could refer to that of the bored pile measured in field; l_i is the thickness of the i-th layer of soil or rock around pile, excluding the length of the expanded section and 2d upward, and d is the diameter of cemented soil pile not expanded.

4.2. Calculation Method for Core Pile Penetration Failure Mode

Considering the similar joints on pile shaft and the same fail mode, the calculation method of cast-in-situ piles with expanded branches and plates can be referred to. The calculation formula for the characteristic value of vertical bearing capacity of the cast-in-situ pile is as follows [14]:

$$Q_u = u_p \sum q_{ski} l_i + \sum \eta q_{pkj} A_{pj} + \eta q_{pk} A_p, \tag{4}$$

where Q_u is the standard value of vertical ultimate bearing capacity of the cast-in-situ pile, u_p is the perimeter of the main pile, q_{ski} is the standard value of ultimate pile shaft resistance in the i-th soil layer, l_i is the effective thickness of the i-th layer of soil or rock around pile excluding the length of branches and plates. q_{pkj} is the resistance of soil beneath the j-th plate, A_{pj} is the j-th plate horizontal sectional area excluding the main pile sectional area, q_{pk} is the tip resistance of the pile, and A_p is the pile tip horizontal sectional area. The second expression in the formula is to calculate the bearing capacity of soil beneath the j-th plate. The coefficient η is related to the position and radium of the plates. According to the analysis of Lu [15], the compaction coefficient of the squeezed branch and plate, β_j = 1.1∼1.3, should also be taken into consideration. The axial force on the upper and lower surface of plates is not the same due to the load borne by the soil beneath the plates directly. In contrast, the nodular joints do not bear the axial force directly [8], so there is no need to derive an expression to calculate the bearing capacity of the joints separately.

Based on the construction mechanism, the standard value of the upper pile shaft resistance q_{sik2} should be greater than the resistance between cemented soil and soil. The upper PRHC or PHC pipe pile shaft resistance is calculated by the method of precast pile.

The lower nodular pile shaft resistance is calculated based on the diameter of the joints. Due to the joints, the axial force declining rate of the nodular piles with depth is faster than that of the PRHC or PHC piles. The compaction coefficient η_2 of nodular joints is related to the length of joints and interval between joints [3]. Compared with cast-in-situ pile with expanded branches and plates, η_2 should be smaller than β_j. Therefore, it is suggested that η_2 = 1.0∼1.1, which is close to the compaction coefficient η_s = 1.05∼1.10 proposed by Zhou [16],

$$Q_{sk2} = u_{ns} \sum q_{sik2} l_i + u_{nx} \sum \eta_2 q_{sik2} l_i, \tag{5}$$

where Q_{sk2} is the standard value of pile shaft resistance in core pile penetration failure mode, u_{ns} is the perimeter of the upper PRHC or PHC pile; q_{sik2} is the standard value of ultimate core pile shaft resistance in the i-th soil layer, the precast pile shaft resistance is taken; u_{nx} is the perimeter of nodular joint, η_2 is the compaction coefficient considering nodular joints, η_2 = 1.0∼1.1, l_i is the thickness of the i-th layer of soil or rock around pile, excluding the length of the expanded section and $2d$ upward, and d is the diameter of the cemented soil pile not expanded.

4.3. Pile Tip Resistance

It is found that, the response of core pile and cemented soil at the expanded section is almost synchronous by the theoretical calculation [2] and numerical simulations [4]. Therefore, it is reasonable to take the nodular pile and the cemented soil at the expanded section as a whole.

For MC pile, the cross section of the whole mixing area is taken to calculate the tip resistance [13]. In addition, the adjustment coefficient of the MC pile tip resistance is ζ = 0.6∼0.8 [13]. Considering the influence of the geological conditions and integrated management, the adjustment coefficient of SDRN pile tip resistance could be taken as η_3 = 0.6.

$$Q_{pk} = \eta_3 q_{bk} A_b, \tag{6}$$

where Q_{pk} is the standard value of pile tip resistance of SDRN pile, η_3 is the coefficient of pile tip resistance, q_{bk} is the standard value of ultimate pile tip resistance, which could refer to that of the precast pile in field; A_b is the sectional area of the expanded section.

In summary, the calculation formulas for the ultimate vertical bearing capacity of SDRN pile are as following:

$$Q_{u1} = Q_{sk1} + Q_{pk}, \tag{7}$$

$$Q_{u2} = Q_{sk2} + Q_{pk}, \tag{8}$$

$$Q_u = \min(Q_{u1}, Q_{u2}). \tag{9}$$

5. Engineering Example Verification

The calculation method proposed by this paper is applied to two SDRN piles in field test to verify the rationality.

5.1. Test Pile Overview and Geological Conditions

In the Ningbo Rail Transit Project, two SDRN piles S2 and S4 are tested in the site. The length of the piles is 64 m and the concrete strength grade of the piles is C80. These two piles adopt the same pile allocation method. The upper section is 15 m PRHC800(130), 15 m PHC800(130)AB, 8 m PHC800(130)AB and 11 m PHC800(130)AB. The lower section of the SDRN pile is PHDC800-600(130). That is, the external diameter of nodular joint is 800 mm, the external diameter of the other section is 600 mm and the thickness of the pipe pile is 130 mm. The borehole diameter is 900 mm. The expanded diameter at pile tip is 1350 mm and the expanded height is 4000 mm. The detailed parameters of test piles are shown in Table 1 and Figure 2. The field soil geological properties and parameters are shown in Table 2.

Table 1. Parameters of test piles.

Number	Diameter	Diameter of the Borehole and Borehole Expanded	Elevation of the Pile Top	Length	Bearing Stratum at the Pile Tip	Load Cell Reading	Distance from Load Cell to Pile Tip
S2, S4	800 mm	900/1350 mm	+4.60 m	64.0 m	⑨$_2$ stratum round gravel	2 × 7800 kN	7 m

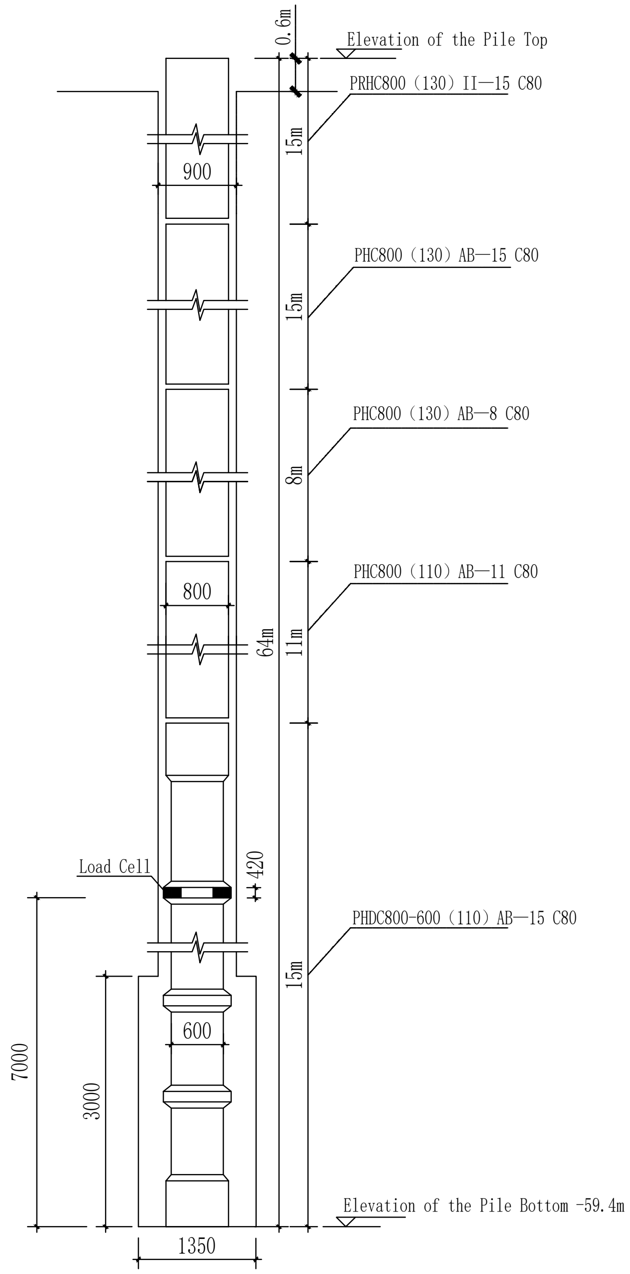

Figure 2. Sketch of the nodular pile.

Table 2. Parameters of the geological borehole.

Number of Soil Layer	Soil Type	Geological Boreholes Q2XZ76		Liquidity Index I_L	Cohesion/kPa	Friction Angle/Deg	Modified Number of SPT N_α [1]	Precast Pile [17]		Slurry Drilling Pile [17]	
		Bottom Elevation/m	Thickness of the Layer/m					q_{sik} [2] /kPa	q_{pk} [3] /kPa	q_{sik} /kPa	q_{pk} /kPa
①$_1$	CL [4]	−1.04	5.00	–	–	–	–	–	–	–	–
①$_2$	CL	−2.19	1.15	0.45	25.8	13.9	10.5	50	–	48	–
②$_2$	CL	−9.04	6.85	1.30	14.8	9.7	–	20	–	18	–
②$_{2b}$	SM [4]	−13.04	4.00	0.95	–	–	7.7	36	–	32	–
②$_3$	CL	−15.04	2.00	1.30	14.1	10.6	4.0	22	–	20	–
④$_1$	CL-ML [4]	−19.04	4.00	1.25	–	–	3.5	22	–	20	–
④$_2$	CL	−27.04	8.00	0.91	18.5	12.1	6.7	46.0	–	42	–
⑤$_1$	CL	−30.34	3.30	0.50	40.6	19.6	41.0	74	2200	70	–
⑤$_5$	GP [4]	−32.44	2.10	–	–	–	58.0	122	7500	115	–
⑥$_1$	CL	−36.04	3.60	0.54	35.8	17.9	20.7	68	–	63	–
⑥$_2$	CL	−39.24	3.20	0.84	25.4	16.4	13.0	52	–	48	–
⑥$_5$	GP	−42.54	3.30	–	3.0	40.0	45.4	150	–	130	–
⑧$_3$	SF [4]	−46.84	4.30	–	3.0	41.0	55.9	115	–	108	–
⑨$_1$	CL	−48.94	2.10	0.42	31.5	20.9	31.3	78	3600	73	–
⑨$_{1a}$	GW [4]	−52.94	4.00	–	3.5	41.0	54.4	150	9000	130	–
⑨$_1$	CL	−57.19	4.25	0.42	31.5	20.9	31.3	78	3600	73	1200
⑨$_2$	GW	−68.80	11.61	–	3.0	43.0	65.5	150	7500	130	1500

[1] $N_\alpha = \alpha N$, α is the correction factors related to the length of the drilling pipe, N is the field number of SPT. [2] q_{sik} is the standard value of the pile shaft resistance. [3] q_{pk} is the standard value of the pile tip resistance. [4] CL is lean clay, SM is silty sand, CL-ML is silty clay, GP is poorly grated gravel, SF is gravel sand, GW is well grated gravel.

5.2. Self-Balanced Load Test Results

The bearing capacity of the piles is tested by self-balanced method in this project. The static tests adopt step-wise loading method [18,19]. The value of each step is approximate to 1/10 of the designed ultimate bearing capacity of the test piles, but the first step is 2/10 of that. Specially, the unloading step is also 2/10 of the designed load. At each load step, the displacement of piles above and under the load cell are recorded every 30 min after each load is applied. The next load is applied until two consecutive displacements within each hour are less than 0.1 mm.

According to the data measured, the load-displacement curves of the two test piles are shown in Figure 3a,b. For S2, when loaded to the 12th level (the load applied is 2 × 7800 kN), the displacements of the piles above and under the load cell are 1.19 mm and 6.94 mm, that of S4 are 6.94 mm and 1.72 mm. When the load is increased to the next step, the displacement of pile increases rapidly. Therefore, the ultimate vertical bearing capacity of the test piles is determined to be the 12th level load. On the basis of coordination principle, the load-displacement ($Q-s$) curves of the piles above and under the loading cell can be transformed into the equivalent load-displacement curve of the pile head in traditional static load test, as shown in Figure 4. According to [20], the ultimate bearing capacity of the test piles can also be worked out, as shown in Table 3.

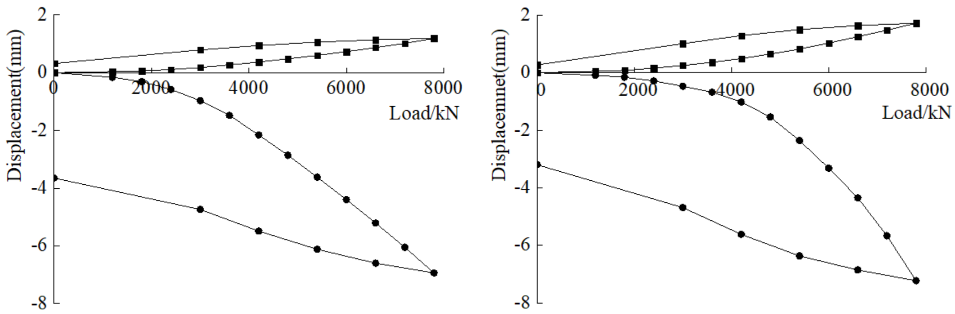

(**a**) (**b**)

Figure 3. Self−balance curves of test piles: (**a**) S2 test pile and (**b**) S4 test pile.

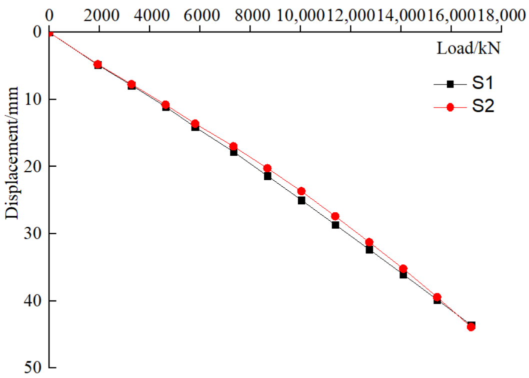

Figure 4. Equivalent transformation curves of S2 and S4.

Table 3. Field test result of the compression bearing capacity Q_u.

Number	Q_{uu}	Q_{lu}	W	γ	Q_u [1]
S2, S4	7800 kN	7800 kN	622 kN	0.8	16,773 kN

[1] $Q_u = \frac{Q_{uu}-W}{\gamma} + Q_{lu}$, where Q_{uu} is the ultimate bearing capacity of pile above load cell, Q_{lu} is the ultimate bearing capacity of pile under load cell, W is the gravity of pile above the load cell, and γ is the conversion factor of the ultimate bearing capacity of pile above load cell.

5.3. Verification of Results

The vertical compression bearing capacity of S2 and S4 is equal considering the same pile allocation method and similar soil condition.

According to the analysis above, two kinds of failure modes may happen. When the test pile is subjected to the overall failure due to insufficient strength of the soil around, the ultimate bearing capacity of the pile is: $Q_{u1} = 16{,}775$ kN ($\eta_1 = 1.05$, $\eta_2 = 1.10$, $\eta_3 = 0.6$). When the test pile is subjected to the core pile penetration failure due to different stiffness of core pile and cemented soil, the ultimate bearing capacity of the pile is: Q_{u2} = 16,492 kN ($\eta_1 = 1.05$, $\eta_2 = 1.10$, $\eta_3 = 0.6$). The ultimate bearing capacity of the single SDRN pile is the smaller one of the two: $Q_u = \min(Q_{u1}, Q_{u2}) = 16,492$ kN.

The result calculated above is close to the ultimate bearing capacity of the test piles measured by self-balanced test in field, which is 16773 kN. Compared with the test result, the calculation result is more conservation, demonstrating the practical significance of the method.

6. Finite Element Simulation by PLAXIS 2D

The foundation responses to external loading are usually studied numerically, analytically, and physically. Due to the unlimited potential, it is found that numerical method is efficient to study practical engineering problems, especially considering the spatial variability of soil. Hu et al. [21] presents a detailed study on the bearing capacity and failure modes of skirted foundation in heterogeneous soil using an h-adaptive FEM. The finite-element results are compared with upper-bound solutions and centrifuge test data to guide further investigation. Johari and Talebi [22] develop a random finite element method (RFEM) to study the influence of spatial variability of soil on the responses of piled-raft foundation. Gholampour and Johari [23] also implement FEM to investigate the effect of heterogeneous soil on soil-structure interaction responses of braced retaining systems. Therefore, the numerical method is of vital importance on the study of the foundation responses and interface behavior under loading. This paper selects PLAXIS 2D for the simulation study.

6.1. Two Dimensional Model

There are two reasons selecting the PLAXIS 2D to simulate the field test. Firstly, it can create boreholes to simulate soil layers in site. Secondly, PLAXIS provides a more comprehensive soil constitutive model than other finite element software. On one hand, the model has axis symmetry. On the other hand, compared with the size of pile and the thickness of stratum, the size of the nodule joint is small. As a result, the PLAXIS 2D model is established to improve the quality of mesh. The ultimate bearing capacity is gotten by applying vertical load to the model pile head step by step. On this basis, the bearing characteristics of the SDRN pile can be analyzed.

In the model, the borehole parameters are input according to Table 2. The parameters of the model pile and cemented soil are input according to Figure 2. To eliminate the boundary effect, the soil model is taken as 7 m in the radial range, and 70 m in the perpendicular direction, approximately at a depth of 5.5 times the diameter of pile below the pile tip, as recommended by Yang and ASCE [24]. The constitutive models are adopted according to the mechanical properties. The pile adopts the linear elastic non-porous model, the cement-soil adopts the Mohr-Coulomb non-porous model, and the soil adopts the Mohr-Coulomb model considering drainage.

In finite element simulation, the result not only depends on the constitutive model selected, but also the properties assigned to the interface between different material. In PLAXIS, the stiffness and strength of the interface depend on the reduction coefficient R_{inter} of the material of less stiffness. For bored piles, R_{inter} of clay is generally taken as 0.8, and R_{inter} of sand is generally 0.7 [25–28]. The mechanical properties of interface between cemented soil and soil are better than that between bored pile and soil. Besides, the friction between pile and cemented soil is much greater than that between cemented soil and soil [29]. Considering the reduction coefficient R_{inter} to be 0.8 and 1.0, two cases of the interface mechanical behaviors are simulated, as shown in Table 4.

Table 4. Three pairs of interfaces and reduction coefficient R_{inter}.

Interface	Core Pile and Cemented Soil	Cemented Soil and Soil	Pile and Soil
Interface modes	From cemented soil	From soil	From soil
$R_{inter,1}$	1.0	1.0	1.0
$R_{inter,2}$	0.8	0.8	0.8

6.2. Simulation Results

Figure 5a–c are the vertical stress distribution of the nodular joints, the cemented soil and the soil around. It can be seen from Figure 5a that, for the upper section (0∼49 m), the axial force of pile and cemented soil are not in the same order of magnitude, which can also be seen from Figure 6a,b. Therefore, in this area, the cemented soil mainly plays the role of transferring load [9–11]. When approaching the joints (49∼64 m), the slope of curve in Figure 6a shows that the decrease speed of pile axial force gets faster. Relevantly in Figure 6b, the axial force of cemented soil has a sudden increase not only at depth of 49 m, but also 61 m, where the expanded cemented soil is. So the nodular joints have contribution to the collaboration work of pile and cemented soil. Under the load at pile head, the axial force of pile tip is 1339 kN, the axial force of expanded soil at the pile tip is 1227 kN. The expanded cemented soil bears about 47.8% of composite pile tip resistance. It indicates that the expanded cemented soil at pile tip plays the role of bearing pile tip resistance.

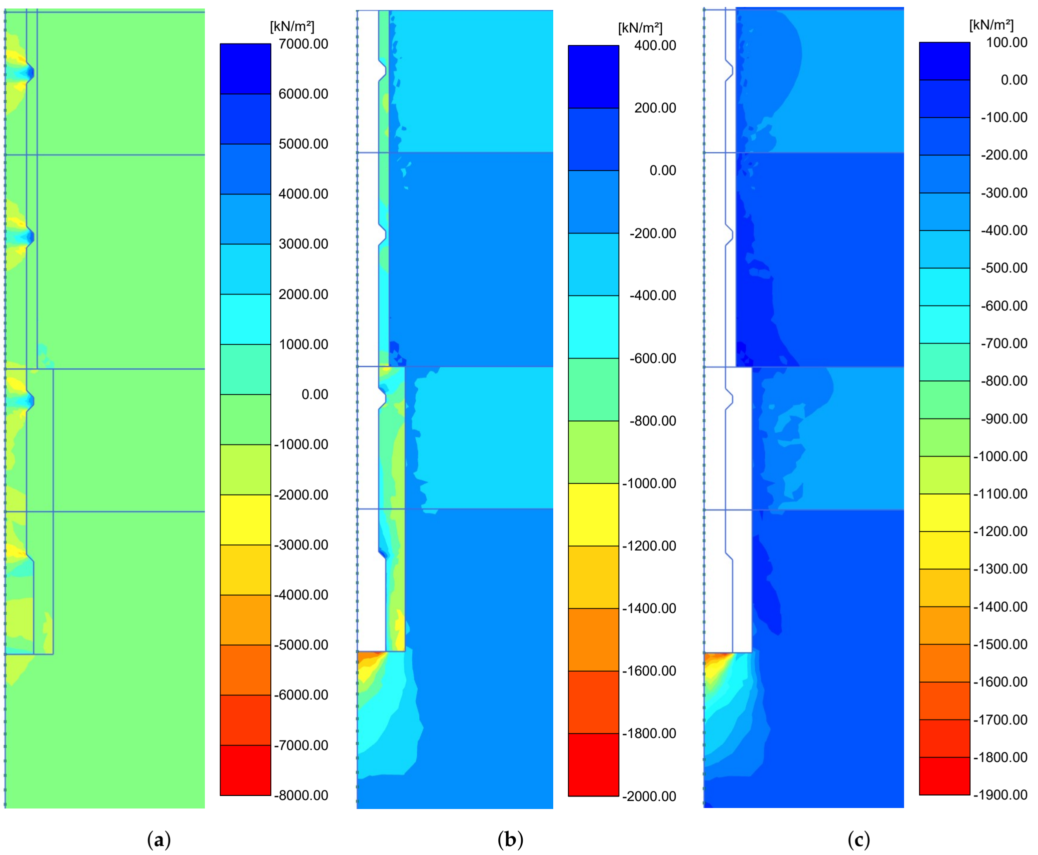

Figure 5. Vertical stress distribution cloud diagrams: (**a**) part of nodular joints, (**b**) cement soil around the joints, and (**c**) soil around the joints.

Figure 7a,b is the plastic point distribution on the interface between cemented soil and soil under the failure mode. From Figure 7a, the distribution of failure point has a difference between soil layers due to different shear resistance. Figure 7b shows that, the failure points not only appear on the interfaces, but also develop upwards from the pile tip. It corresponds to Figure 6b. This is because the expanded cemented soil tip exposes to a large tip load. Therefore, to ensure the collaborative work of pile tip and expanded cemented soil, it is necessary and economical to strengthen the cemented soil in this specific area considering the bearing capacity of the soil layer at the pile tip.

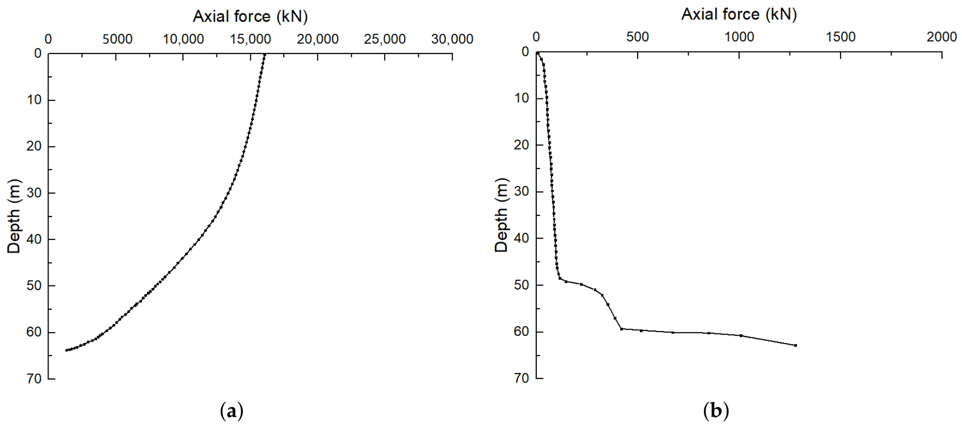

Figure 6. Axial force—Depth curves of (**a**) piles, and (**b**) cemented soil.

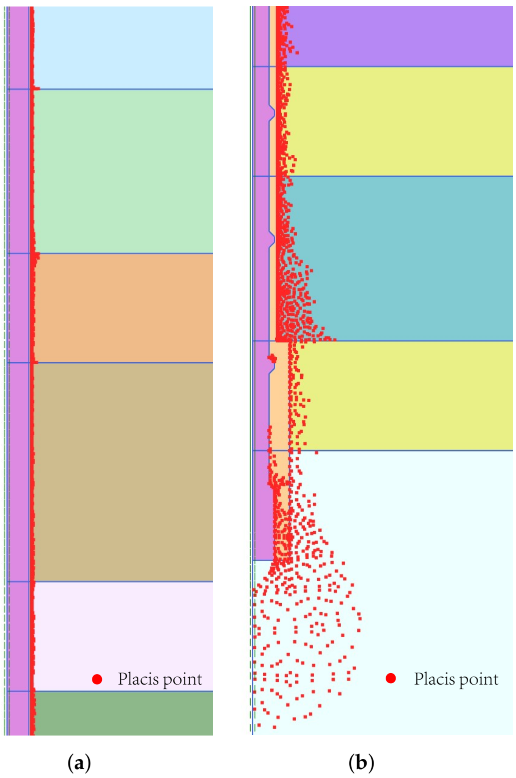

Figure 7. Plastic point distribution diagrams among (**a**) pile shaft, and (**b**) pile tip.

The load-displacement simulation curves of piles in the cases of $R_{inter,1}$ and $R_{inter,2}$ are shown in Figure 8. The load is set to be 2000 kN for each stage in the initial loading stage, and 1000 kN for each stage in the later stage. The load corresponding to the starting point of obviously steep drop is the ultimate bearing capacity. It can be seen from the curve that when the strength reduction of interface is not taken into consideration, Q_{ua} = 16,100 kN.

When the strength reduction of interface is taken into consideration, Q_{ub} = 12,800 kN. The simulation result without considering the strength reduction are closer to the field test result. Therefore, it is confirmed that the SDRN pile method can improve the friction resistance of the interfaces. In addition, Table 5 indicates that the finite element model and the calculation method in this paper are feasible for SDRN pile.

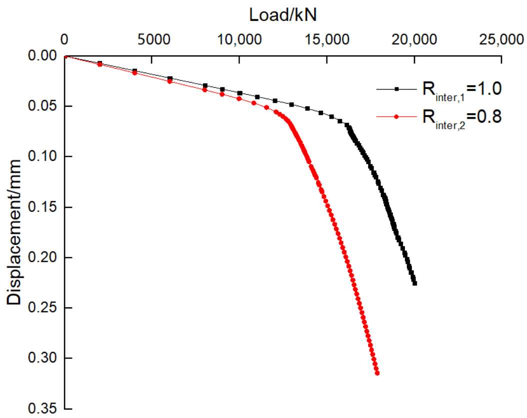

Figure 8. Load–Displacement simulation curves of piles with $R_{inter,1}$ and $R_{inter,2}$.

Table 5. Vertical bearing capacity of SDRN pile by field test, theory calculation, and simulation.

Methods	Field Test	Proposed Calculation Method	Finite Element Simulation
Results	16,773 kN	16,492 kN	16,100 kN

7. Limitations and Future Works

This paper proposes a calculation method for ultimate vertical bearing capacity of SDRN pile considering two failure modes. The calculation result is compared with the field test result and numerical simulation result by PLAXIS. Some valuable conclusions concerning the pile responses are derived. However, there are also some limitations in this paper:

- This paper derives the calculation method from that of similar common pile foundation mainly considering the construction technology. However, the shear strength on the interface between cemented soil and soil is also of vital importance for the bearing capacity, which is related to the mechanical properties of the cemented soil. The coefficient could also take this into consideration.
- One or two more field tests could be implemented to support this calculation method more forcefully by changing the thickness of cemented soil around the pile.

Therefore, several further investigations on the pile responses could be conducted. Some laboratory experiments could be designed for the shear strength parameters of cemented soil. Field tests concerning the collaborative work between cemented soil and soil both along the pile shaft and in the expended cemented soil area at the pile tip also need to be carried out. Finally, this paper is focus on the vertical bearing capacity of SDRN pile, the horizontal bearing characteristic is also of vital study value.

8. Conclusions

In this paper, the calculation method for the ultimate compression bearing capacity of SDRN pile considering two kinds of failure modes is proposed. The following conclusions can be obtained:

- When the core pile and cemented soil shell fail as a whole, the standard value of ultimate pile shaft resistance should be calculated by the perimeter of the cemented soil pile. The ultimate shear resistance provided by each soil layer around the pile

is approximate 1.05∼1.10 times that of the bored pile. When the pile and cemented soil shell have a relative displacement, the standard value of the ultimate pile shaft resistance should be calculated by the perimeter of the composite pile. The ultimate shear resistance provided by each soil layer could take the displacement pile shaft resistance. The lower section should consider the squeezing effect of the nodular joints;
- When calculating the SDRN pile tip resistance, it is necessary to consider not only the expanded cemented soil approaching the pile tip, but also the geological conditions and the integrated management. So the precast pile tip resistance is referred to, the adjustment coefficient of SDRN pile tip resistance could be taken as $\eta_3 = 0.6$;
- In the numerical calculation, when the interface strength reduction coefficient R_{inter} is taken as 1.0, the calculation result are more close to the field test result. Therefore, compared with the general bored piles, the mechanism properties of interfaces between SDRN pile and cemented soil, cemented soil and soil are better. In addition, both the nodular joints and the expanded cemented soil can improve the bearing capacity of the pile foundation;
- Based on the pile parameters and soil parameters in the project, the ultimate compression bearing capacity of SDRN pile calculated by the theoretical method and the finite element method proposed in this paper are close to that in field, providing a practical reference.

Author Contributions: J.G.: Methodology, writing (original draft). Y.W.: data curation. G.D.: conceptualization, writing (review and editing). All authors have read and agreed to the published version of the manuscript.

Funding: This research was funded by National Natural Science Foundation of China [grant number 52078128].

Institutional Review Board Statement: Not applicable.

Informed Consent Statement: Not applicable.

Data Availability Statement: Not applicable.

Acknowledgments: The authors would like to express appreciation to the editors and reviewers for their valuable comments and suggestions. The authors are grateful for the support by the National Natural Science Foundation of China [grant number 52078128].

Conflicts of Interest: The authors declare no conflict of interest. The funders had no role in the design of the study, in the collection, analyses, or interpretation of data, in the writing of the manuscript, or in the decision to publish the results.

References

1. Xu, L. Research on the Bearing Capacity and One Dimension Wave Characteristic of Static Drill Rooted Nodular Piles. Ph.D. Thesis, Zhejiang University, Zhejiang, China, 2015.
2. Qiong, Y. Research on the Vertical Compression Bearing Capacity of Static Drill Rooted Nodular Piles. Ph.D. Thesis, Zhejiang University, Zhejiang, China, 2015.
3. Zhou, J. Tests and Numerical Simulation on the Bearing Capacity and Settlement of Static Drill Rooted Nodular Piles. Ph.D. Thesis, Zhejiang University, Zhejiang, China, 2015.
4. Qian, Z. Experimental Study and Numerical Analysis of Bearing Capacity of Static Drill Rooted Nodular Piles. Ph.D. Thesis, Zhejiang University, Zhejiang, China, 2015.
5. Yang, M. Research on the Compression and Uplift Bearing Capacity of Drill Rooted Grouting Nodular Piles. Ph.D. Thesis, Zhejiang University, Zhejiang, China, 2013.
6. Zhou, J.; Wang, K.; Gong, X.; Zhang, R. Bearing capacity and load transfer mechanism of static drill rooted nodular piles. *Rock Soil Mech.* **2014**, *35*, 1367–1376.
7. Zhou, J.; Gong, X.; Wang, K.; Zhang, R.; Research Center of Coastal and Urban Geotechnical Engineering, Zhejiang University; ZDOON Building Material Group. Performance of static drill rooted nodular piles under compression. *J. Zhejiang Univ. Eng. Sci. Ed.* **2014**, *48*, 835–842.

8. Gong, X.; Xie, C.; Shao, J.; Shu, J.; Research Center of Coastal and Urban Geotechnical Eng., Zhejiang Univ.; Key Lab. of Soft Soils and Geoenvironmental Eng., Ministry of Education, Zhejiang Univ.; ZCONE High-tech Pile Industry Holdings Company Limited. Analysis of Bearing Characteristics of the Static Drill Rooted Nodular Piles under Tension and Compression. *J. Sichuan Univ. Eng. Sci. Ed.* **2018**, *50*, 102–109.
9. Zhang, R.; Wu, L.; Kong, Q. Analysis of Bearing Characteristics of the Static Drill Rooted Nodular Piles under Tension and Compression. *J. Sichuan Univ. Eng. Sci. Ed.* **2013**, *35*, 1200–1203.
10. Gong, P. Load Transfer Mechanism of Concrete-Cored DCM Pile. Ph.D. Thesis, Chinese Academy of Sciences, Guangzhou, China, 2004.
11. Zhou, J.; Wang, K.; Gong, X.; Zhang, R. Bearing capacity and load transfer mechanism of a static drill rooted nodular pile in soft soil areas. *J. Zhejiang Univ. Eng. Sci. Ed.* **2013**, *14*, 705–719. [CrossRef]
12. Zhang, R.; Chen, H.; Wu, L.; Li, W.; Wang, S. *Technical Specification for Static Drill Rooted Nodular Piles*; Ningbo Zhedong Foundation Engineering Corporation: Ningbo, China, 2011; p. 10.
13. Deng, Y.; Peng, X.; Hu, M.; Wang, A.; Xu, B.; Qian, Y.; Lu, H.; Wang, J.; Hua, M.; Wei, J.; et al. *Technical Specification for Strength Composite Piles*; Construction Office of Jiangsu Province: Nanjing, China, 2013; pp. 9–11.
14. Tang, Y.; Zhang, X.; Cui, J.; Han, S.; Yang, G.; Xue, H.; Miao, Q.; Yang, S.; Li, X.; Zhang, G. *Technical Specification of Cast-in-Place Piles with Branches and Plates*; China Construction Industry Press: Beijing, China, 2006; pp. 11–13.
15. Lu, C.; Meng, L.; Wang, Z.; Zhou, Q. Test of model piles with branches and plates in unsaturated silty clay. *Chin. J. Geotech. Eng.* **2004**, *26*, 522–525.
16. Zhou, J.; Gong, X.; Wang, K.; Zhang, R.; Yan, T.; Research Center of Coastal and Urban Geotechnical Engineering, Zhejiang University; ZDOON Building Material Group. Application of static drill rooted precast nodular pile in soft soil foundation and calculation for bearing capacity. *Chin. J. Rock Mech. Eng.* **2014**, *33*, 4359–4366.
17. Huang, Q.; Jin, L.; Gao, W.; Jin, B.; Sha, Z.; Hou, W.; Qiu, M.; Gu, X.; Chun, L.; Gu, G.; et al. *Technical Code for Building Pile Foundation*; China Construction Industry Press: Beijing, China, 2008; pp. 19–21.
18. Chen, F.; Xu, T.; Zhu, G.; Zhong, D.; Liu, M.; Liu, J.; Ye, W.; Teng, Y.; Li, D.; Liu, Y.; et al. *Technical Code for Testing of Building Foundation Piles*; China Construction Industry Press: Beijing, China, 2014; pp. 15–16.
19. Gong, W.; Xue, G.; Dai, G.; Tong, X.; Mu, B. *Static Loading Test of Foundation Pile—Self-Balanced Method*; China Communications Press: Beijing, China, 2009; p. 4.
20. Gong, W.; Mao, L.; Gao, Q.; Xue, G.; Dai, G.; Tong, X.; Mu, B. *Technical Specification for Static Load Testing of Self-Balanced Method of Foundation Pile*; Jiangsu Science and Technology Press: Nanjing, China, 2020; pp. 13–15.
21. Hu, Y.; Randolph, M.F.; Watson, P.G. Bearing response of skirted foundation on nonhomogeneous soil. *J. Geotech. Geoenvironmental Eng.* **1999**, *125*, 924–935. [CrossRef]
22. Gholampour, A.; Johari, A. Reliability-based analysis of braced excavation in unsaturated soils considering conditional spatial variability. *Comput. Geotech.* **2019**, *115*, 103163. [CrossRef]
23. Johari, A.; Talebi, A. Stochastic analysis of piled-raft foundations using the random finite-element method. *Int. J. Geomech.* **2021**, *21*, 04021020. [CrossRef]
24. Yang, J.; Asce, M. Influence Zone for End Bearing of Piles in Sand. *J. Geotech. Geoenviron. Eng.* **2006**, *132*, 1229–1237. [CrossRef]
25. Kim, Y.; Jeong, S. Analysis of soil resistance on laterally loaded piles based on 3D soil–pile interaction. *Comput. Geotech.* **2011**, *38*, 248–257. [CrossRef]
26. Xue, F.; Ma, J.; Yan, L. Three-dimensional FEM analysis of bridge pile group settlement in soft soils. *Adv. Pile Found. Geosynth. Geoinvestig. Found. Fail. Anal. Repairs* **2011**, *220*, 135–143. [CrossRef]
27. Khelifi, Z.; Berga, A.; Terfaya, N. Modeling the Behavior of Axially and Laterally Loaded Pile with a Contact Model. *Electron. J. Geotech. Eng.* **2011**, *16*, 1239–1258.
28. Huang, T.; Yang, C. Side friction of drilled piles in cobble layers. *J. Mar. Sci. Technol.* **2016**, *24*, 143–151.
29. Xie, C. Numerical study on behavior of pre-bored grouting plated nodular pile under compressive and tension. Ph.D. Thesis, Zhejiang University, Zhejiang, China, 2018.